Environ. Sci. Technol. **2000**, *34,* 1671−1678

Complete Compositional Monitoring of the Weathering of Transportation Fuels Based on Elemental Compositions from Fourier Transform Ion Cyclotron Resonance Mass Spectrometry

RYAN RODGERS,[‡] ERIN N. BLUMER,[‡] MICHAEL A. FREITAS,[‡] AND ALAN G. MARSHALL*,[†]

National High Magnetic Field Laboratory at Florida State University, 1800 East Paul Dirac Drive, Tallahassee, Florida 32310, and Department of Chemistry, Florida State University, Tallahassee, Florida

We have determined elemental compositions for hundreds of components of diesel fuel, jet fuel (JP-8), and gasoline and characterized each of their chemical compositions before and after artificial "weathering" (i.e., evaporation to a specified fraction of the original weight). An all-glass heated inlet system (AGHIS) coupled to a home-built 6.0 T Fourier transform ion cyclotron resonance (FT-ICR) mass spectrometer provides ultrahigh mass resolving power ($m/\Delta m_{50\%} > 100\,000$, in which $\Delta m_{50\%}$ is the full peak width at half-maximum peak height) and sufficiently high mass accuracy (≤0.8 ppm) for unique identification of all chemical components. A 1 μL septum injection of each weathered/unweathered transportation fuel into the AGHIS yields a mass spectrum containing 100−500 peaks, $50 \leq m/z \leq 300$, with as many as five peaks (of different elemental composition) at a given nominal mass. Elemental composition assignment of every peak in the mass spectrum of each fuel and its weathered analogues provides a unique chemical "fingerprint" that serves to identify positively the contaminant and quantitate the extent of weathering. Weathered jet and diesel fuels (and gasoline to a lesser extent) exhibit a significant shift in the relative abundance to higher-mass ($m/z \geq 200$) species, in accord with prior gas chromatographic (GC) evidence for a shift toward increased retention time with increased degree of weathering.

Introduction

The United States' heavy dependence on fossil fuels necessitates transportation of large volumes of commercial fuels via pipeline, ships, rail, and tractor-trailers. In addition, a highly developed infrastructure of highways, interstates, railways, and shipping channels supports an enormous volume of international and interstate commerce. A combination of the large volumes of hydrocarbons consumed in the U.S.A. (*1*) and the methods used to transport them lead to the loss of large amounts of commercial fuels into the environment through various accidents, leaks, or intentional discharge. Whether by pipeline ruptures, supertanker accidents, leaking underground storage tanks, or other sources, hydrocarbon contamination represents a common, major source of soil and groundwater contamination. For example, underground storage tanks alone were estimated by the United States Environmental Protection Agency to account for approximately 1.5 million leaking sites in the United States in 1993. Furthermore, the extent of contamination varied widely among the sites: approximately 40% of those 1.5 million tanks leaked badly enough to contaminate underlying groundwater.

Once released into the environment, the fuel undergoes various physical and chemical processes that contribute to its migration, removal, and modification (*2*−*6*). Physical processes such as volatilization, washout, and sorption can occur very rapidly after contaminant introduction, targeting specific classes of compounds. Compounds having a low boiling point are lost quickly through volatilization and water-soluble compounds such as benzene, toluene, ethylbenzene, and xylene (BTEX compounds) are lost to washout. Volatilization and washout are of primary importance since both increase the mobility of the contaminant, thereby increasing the risk of human exposure and subsequently, adverse health effects (*2, 3, 7, 8*). Analytical methods for such analyses are well established and quite routine due to the absence of matrix contributions from the environment in which the fuel was lost. For washout studies, simple liquid−liquid extractions can be performed on collected water samples at the site or modeled in the lab for a reasonable assessment of water soluble components (*9*−*11*). Volatilization studies have been simplified through the use of purge and trap and solid-phase microextraction (SPME) techniques that eliminate environmental matrix contributions except for the most volatile soil components (*12*−*16*).

Although volatile and highly soluble components of the fuel present the greatest immediate health risk, compositional information of the residual fraction as it ages is important for understanding of leaching characteristics and continued contaminant volatilization (*1, 17, 18*). Typical gas chromatograph (GC) or GC-mass spectrometry characterization techniques suffer from a lack of both chromatographic and mass spectral resolution in the analysis of aged petroleum fuels or oils (*14, 19*−*24*). Researchers typically describe an "unresolved complex mixture" or UCM in efforts to characterize aged petroleum and or transportation fuel spills (*25*−*35*). After extended time in the soil, chemical and biochemical modifications begin to modify the remaining contaminants. Both photooxidation and bioremediation increase the component diversity of an already complex mixture. Identification of individual constituents that comprise the mixture becomes exceedingly difficult and beyond the analytical capabilities of current GC and GC-MS instruments. Elaborate sample preparation schemes have been devised to overcome the complexity of the hydrocarbon mixture but still suffer from insufficient resolution, lack of reference compounds, and sample loss or dilution due to a second separation stage (*36*−*40*).

Fourier transform ion cyclotron resonance mass spectrometry (FT-ICR MS) offers ultrahigh mass resolving power ($>1 \times 10^6$), sub ppm mass accuracy, and simultaneous broadband analysis in a few seconds (*41*−*48*), making it an attractive option for complex volatile mixture analysis with little or no sample preparation (*49*−*51*). Routine ultrahigh mass resolving power ($m/\Delta m_{50\%} > 100\,000$, in which $\Delta m_{50\%}$

* Corresponding author phone: (850)644-0529; fax: (850)644-1366; e-mail: marshall@magnet.fsu.edu.

[†] National High Magnetic Field Laboratory at Florida State University.

[‡] Florida State University.

10.1021/es990799i CCC: $19.00
Published on Web 03/15/2000

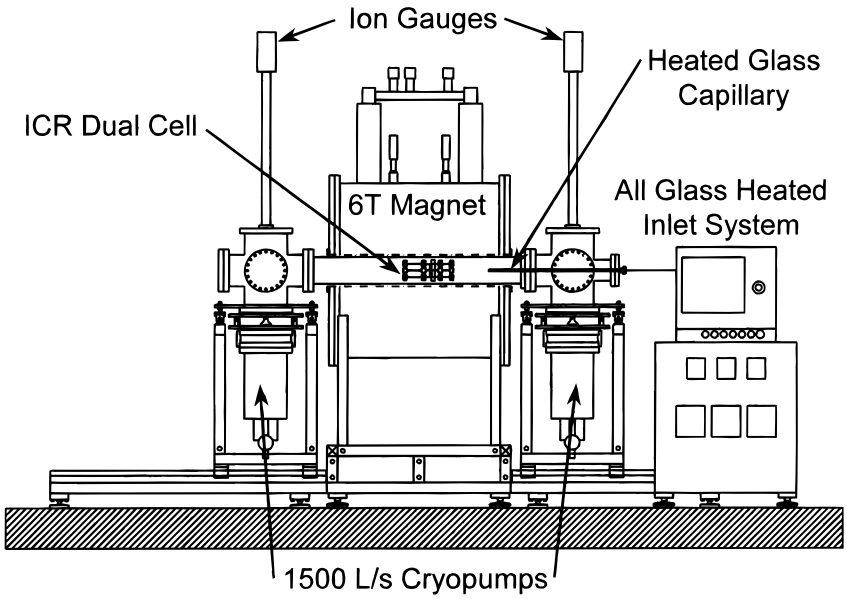

FIGURE 1. Schematic diagram of a 6.0 T Fourier transform ion cyclotron resonance mass spectrometer coupled to an all-glass heated inlet system (AGHIS) via a heated glass capillary for volatile mixture analysis.

is the mass spectral full peak width at half-maximum peak height) for volatile and semivolatile organic molecules allows for the baseline resolution of multiple peaks at a given nominal mass. Sub ppm mass accuracy allows for the unambiguous assignment of molecular formulas (elemental compositions) based on accurate mass measurement alone for molecules up to several hundred Dalton. High resolution and high mass accuracy allow for both resolution and identification of hundreds of components present in commercial fuels in a single scan (*49*, *51*).

Here we report an environmental application of FT-ICR mass spectrometry to the complete compositional analysis of three transportation fuels and their "weathered" (i.e., evaporated to a specified fraction of their original weight) analogues. Changes in the mass spectrum yield compositional information about the weathering process and identify those species that most resist volatilization and therefore dominate the residual fraction left in the soil. Difference mass spectra make it easy to visualize compositional changes as a function of weathering and offer potential for the identification of complex organic mixtures based on high-resolution mass spectrometric compositional inventory.

Experimental Section

All experiments were carried out on a home-built FT-ICR mass spectrometer equipped with a horizontal 15 cm diameter room bore 6 T magnet (Oxford Corp.) and a modular ICR data station (MIDAS) (*52*). Briefly, the mass spectrometer features dual (*53*) closed (by circular solid disk end caps) perforated cylindrical Penning ion traps and is evacuated by a pair of 1500 L/s (N_2) cryopumps (CryoTorr 8, CTI Cryogenics, Mansfield, MA). The mass spectrometer, shown in Figure 1, is connected to an All-Glass Heated Inlet System (AGHIS) (R. J. Brunfeldt Company) by a resistively heated glass transfer line (0.5 mm i.d.) (*54*). Sample introduction into the AGHIS can be made by one of two methods. Samples can either be injected through a septum or placed in an ampule before introduction to the heated expansion volume maintained at 250 °C. Once volatilized, sample gas was leaked through a glass transfer line containing a drawn glass conductance limit (~80 μm i.d.) prior to introduction to the source high vacuum chamber. The sample path was designed entirely of glass to ensure that no catalytic cracking results from contact with a hot metal surface, and the transfer/introduction capillaries are maintained at 200 °C to prevent sample condensation.

Ionization, ion transfer, excitation/detection, and data manipulation are identical to those previously reported (*55*). Briefly, the volatilized sample was ionized by 18 eV electrons (50−500 ms beam duration) and the trapping potential successively lowered from 2 to 0.4 V prior to broadband chirp excitation (100−1.56 MHz) at a sweep rate of 1×10^9 Hz/s and ~21 V_{p-p} excitation voltage. The resulting time-domain data (2 MB) were Hanning-apodized prior to a single zero-fill followed by fast Fourier transform, magnitude calculation, and frequency-to-mass conversion (*56*) to generate a final m/z spectrum. Likewise, assignment of molecular formulas and calibration procedure were also as previously reported. In short, the spectra were externally calibrated from a standard 10-component mixture of alkyl aromatic hydrocarbons (*50*). After unequivocal molecular formula assignment of standard species bracketing the mass range of interest, an internal calibration was based on peaks unambiguously identified from the external calibration. The internal calibration coefficients were applied to the standard 10-component hydrocarbon mixture to verify the internal calibration. (External and internal calibration here denote mass calibration (horizontal axis of the mass spectrum), not sensitivity calibration (vertical axis).)

Jet fuel (JP-8) was obtained from Eglin Air Force Base (Fort Walton Beach, FL) and used as an unweathered standard. Unweathered/artificially weathered diesel fuel and gasoline standards were obtained from Restek Corp. (Bellefonte, PA) as neat liquids and were prepared by the method described below. Artificially weathered JP-8 standards were prepared from the unweathered JP-8 standard as follows. Aliquots of the unweathered fuel were transferred to glass vials and placed under a gentle stream of dry nitrogen. Percent weathering was determined by weight loss (i.e. 50% weathered JP-8 had lost 50% of its initial weight) for 25, 50, 75, 85, and 95% weathered jet fuel. The resulting fuel was stored at 4 °C, then removed, warmed to room temperature, and injected (1 μL injection volume) into the septum inlet of the AGHIS for analysis.

Results and Discussion

Unweathered/Weathered Diesel Fuel. A 1 μL aliquot of the unweathered diesel fuel injected into the septum inlet of the

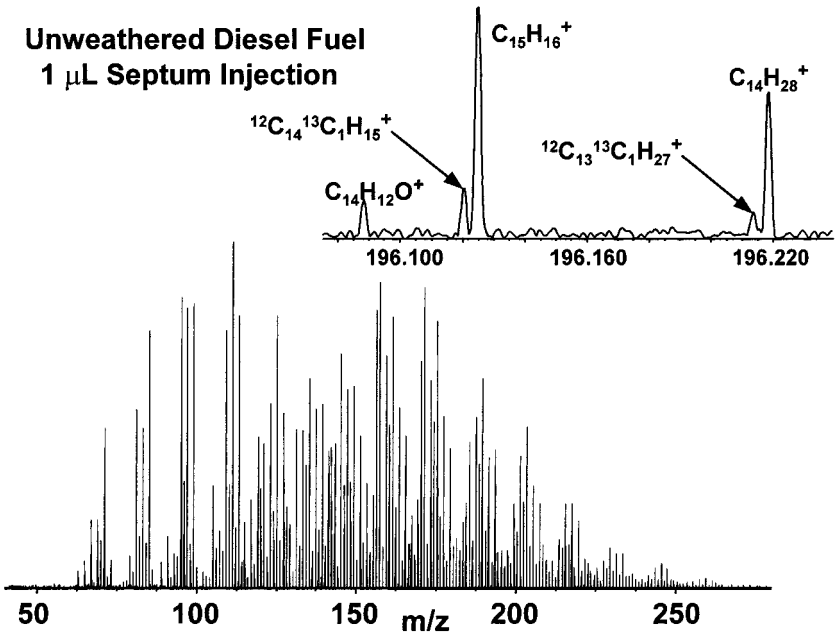

FIGURE 2. Full-range FT-ICR mass spectrum (bottom) and a mass scale-expanded segment (inset) for an unweathered diesel fuel sample resulting from a 1 μL septum injection into the AGHIS. Note the baseline resolution of five components present at the same nominal mass, at a mass resolving power ($m/\Delta m_{50\%}$) $\approx$ 100 000, in which $\Delta m_{50\%}$ is the mass spectral peak full width at half-maximum peak height. Elemental compositions are assigned to every peak in this and all the following mass spectra based only on accurate mass measurement with an average mass error of 0.8 ppm.

AGHIS provided a stable source pressure of $\sim 3 \times 10^{-9}$ Torr for 1 h. The ultrahigh-resolution (mass resolving power ($m/\Delta m_{50\%} \approx 100\,000$, in which $\Delta m_{50\%}$ is the full peak width at half-maximum peak height) FT-ICR mass spectrum consisted of $\sim$500 peaks (Figure 2, bottom) over the mass-to-charge ratio range, $50 \leq m/z \leq 300$, with as many as five peaks at each individual nominal mass. (Essentially no multiply charged ions were present, as evidenced by absence of peaks at 1/2, 1/3, etc. of adjacent nominal m/z values. We shall therefore refer interchangeably to mass or m/z from here on.) A mass scale-expanded segment (Figure 2, top) illustrates the complexity of the spectrum, with five baseline-resolved peaks (corresponding to five different elemental compositions) at the same nominal mass. After mass calibration, elemental compositions were assigned based on accurate mass measurement alone with an average mass error of 0.7 ppm. It should be noted that, for practical purposes, mass measurement alone cannot distinguish geometric isomers, because their rest masses typically differ by less than 10^{-11} Da. Thus, for example, $C_{15}H_{16}$ in Figure 2 could be either C_3 acenaphthalene or C_3 biphenyl.

Figure 3 shows broadband mass spectra of 25% (top left) and 75% (bottom left) weathered diesel fuel, along with mass scale-expanded segments, $250 \leq m/z \leq 300$ (top right and bottom right), revealing compositional changes as a result of weathering. Specifically, there is a marked shift in the relative abundance toward high-mass ($m/z \geq 250$) components with increased weathering. The shift is evident from the broadband mass spectra (compare to Figure 2) but is more obvious from the zoom mass insets. Elemental composition assignment of all peaks in the mass spectra from unweathered, 25, 50, and 75% weathered samples allows for direct monitoring of compositional changes in the fuels and results in a unique elemental composition "fingerprint" that can be used for positive identification of the unweathered fuel and/or its weathered analogues.

Quantitation of Weathering. A difference spectrum calculator program in the MIDAS data analysis package quantitates compositional changes on weathering. First, the program searches for the analyte (in this case, weathered fuel) peak whose m/z matches the m/z of each reference (unweathered fuel) peak to within the experimentally determined mass accuracy (e.g., 1 ppm in the present example). (Analyte peaks that have no match in the reference are outputted separately, because in soil-extracted weathered fuel, additional species not present in the original unweathered fuel may be present, and we do not want such species to interfere with our measure of weathering of the original fuel.) Second, in order that the difference spectrum does not simply reflect differences in ion *absolute* abundances between analyte and reference samples, each m/z spectrum is vertically scaled to the sum of the magnitudes of *all* of the above-threshold peaks in that spectrum. A difference spectrum (Figure 4) is then generated by subtracting the mass spectral peaks present in the reference spectrum from those of the analyte spectrum. The idea here is that if each peak were scaled relative to the largest peak in a spectrum, and if only the largest peak changes its amplitude (on weathering, in this case), then there would be large-amplitude peaks throughout the difference spectrum, even though most of the component abundances did not change. Therefore, we prefer to scale each peak height to the sum of all peaks, to better reflect global (rather than just a few) differences between two spectra.

To quantitate the agreement between sample and reference spectra, we define a "difference" score as the least-squares deviation for the difference spectrum: the lower the score, the better the match between the analyte and the reference. Positive peaks in the difference spectrum obviously result for the following: (a) compounds present in the analyte but either absent or at lower abundance in the reference or (b) compounds present at higher abundance in the analyte relative to the reference spectrum. Likewise, negative peaks in the difference spectrum result for the following: (a) compounds present in the reference but either absent or at lower abundance in the analyte or (b) compounds present in greater abundance in the reference than in the analyte spectrum. The advantage of the normalization method of the preceding paragraph is that the difference spectrum (after excluding peaks not present in the original reference

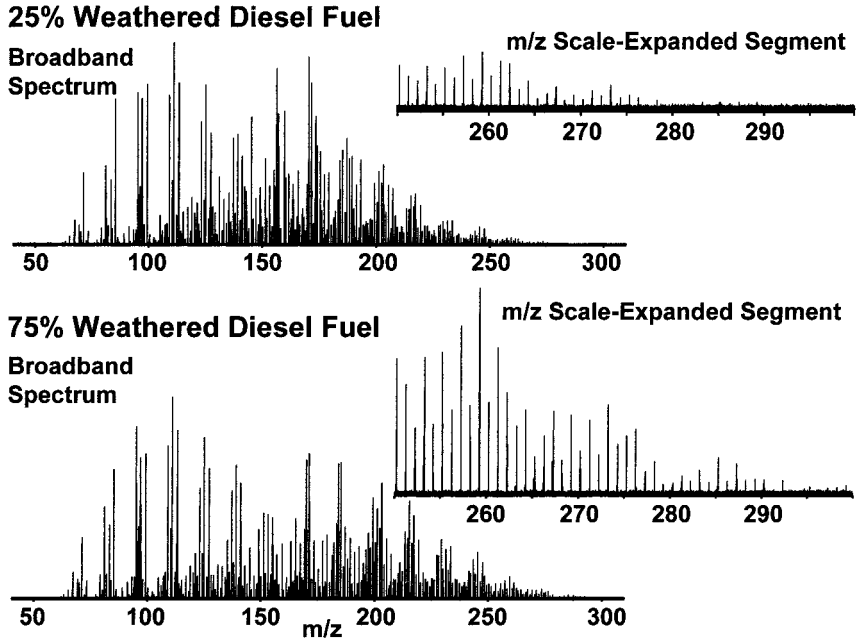

FIGURE 3. Full-range FT-ICR mass spectra of 25% (top) and 75% (bottom) weathered diesel fuel and mass scale-expanded segments (250 ≤ *m/z* ≤ 300) (inset above each broadband spectrum) showing that weathering results primarily in loss of lower-mass species, resulting in a dramatic increase in the relative abundance (and number) of high *m/z* species. The noise level has been scaled to approximately the same noise level in each zoom mass inset so as to illustrate the increase in relative abundance of species falling between 250 ≤ *m/z* ≤ 300 as a function of increased weathering.

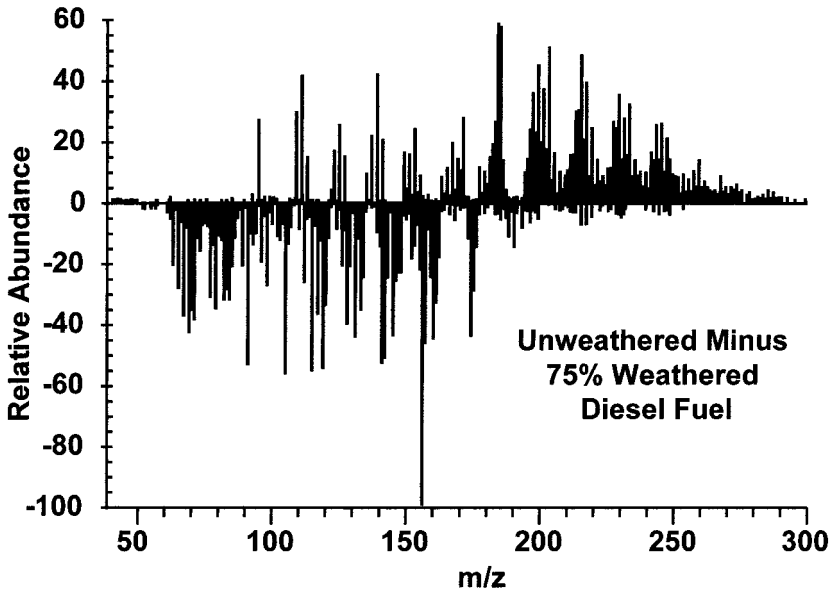

FIGURE 4. Difference FT-ICR mass spectrum between 75% weathered diesel fuel and unweathered diesel fuel (each spectrum is scaled according to the sum of all above-threshold peak magnitudes before computing the difference spectrum) Weathering clearly results in partial or complete removal of low-mass species (negative peaks), leaving mainly high-mass species at higher relative abundance (positive peaks).

spectrum) will have the (desirable) property that the sum of all of the positive-peak magnitudes will be the same as the sum of the negative-peak magnitudes. Thus, the least-squares difference score will depend only on true differences in composition between analyte and reference and not on which peak happens to have the highest relative abundance.

The difference spectrum (Figure 4) for weathered minus unweathered diesel fuel clearly demonstrates the shift in relative abundance from low m/z species (negative peaks in the difference spectrum) to higher-mass species (positive peaks in the m/z difference spectrum) as a result of prolonged weathering. The negative peaks indicate peaks present in the unweathered diesel fuel but not present or attenuated in the 75% weathered diesel fuel. Likewise, positive peaks denote peaks present in the 75% weathered but at lower relative abundance in the unweathered diesel fuel. A similar shift (at vastly lower resolution) is also observed in gas chromatographic analyses of other commercial transportation fuels and is attributed to the preferential vaporization of the low boiling point components of the fuel as result of weathering. In mass spectral analysis, the shift is manifested (Figures 2−4) in a shift in relative abundance to higher m/z on weathering, because the boiling points for most classes of compounds present in the fuels vary approximately inversely with molecular weight.

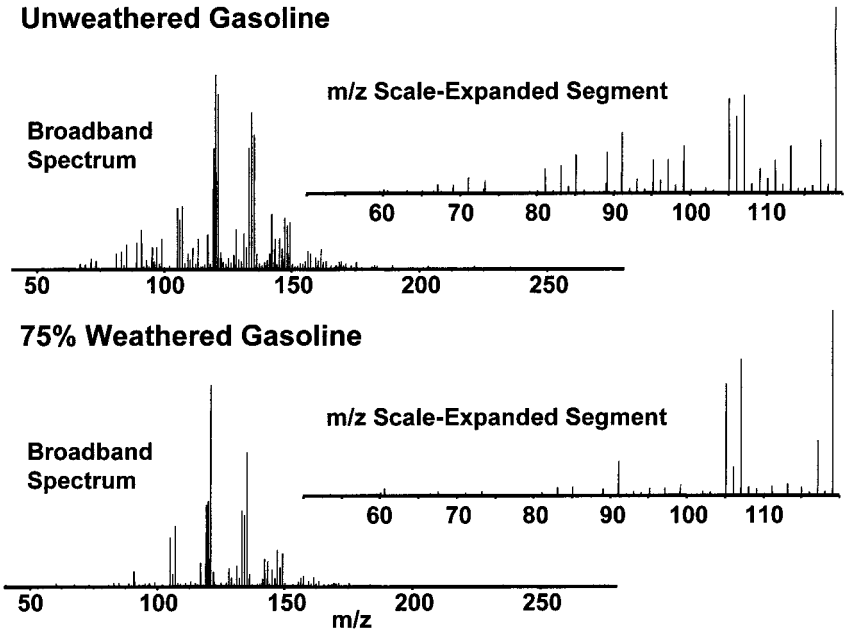

FIGURE 5. Full-range FT-ICR mass spectra of unweathered (top) and 75% weathered (bottom) gasoline. Note the much simplified composition compared to diesel fuel, consisting mostly of a single peak at every nominal mass but with as many as four peaks present at some *m/z* values. A zoom mass inset ($50 \leq m/z \leq 120$) above each broadband spectrum further illustrates the relatively simple distribution of components. Prolonged weathering results in preferential evaporation of lower-mass components.

Both the positive and negative peak distributions in the weathered minus unweathered m/z difference spectrum show periodic variation, i.e., groups of peaks spaced ~14 Da apart, presumably due to series of derivatives differing by number of methylenes (CH_2). Interestingly, the weathered minus unweathered difference spectrum contains several groups of negative peaks located *between* groups of positive peaks at high m/z. Thus, more than just mass determines volatility: at least some high-mass species remain after weathering, even though other comparably high-mass species are removed. It appears that volatility decreases with increasing molecular weight within a given molecular class and that there are multiple overlapping classes of compounds. Tandem mass spectrometry (MS/MS) experiments (*57*−*59*) should help to identify additional structural features (rings, chains, isomers, etc.) of the weathered vs unweathered components.

One should be aware that, even at the relatively low electron energy (18 eV) of the present experiments, most paraffins will be highly fragmented. In contrast, alkyl aromatics tend to yield molecular ions. Therefore, the present mass spectra may emphasize aromatics over saturates and may not accurately reflect overall hydrocarbon compositions.

Unweathered/Weathered Gasoline. A 1 μL septum injection of unweathered/weathered gasoline into the AGHIS led to a stable base pressure of $\sim 9 \times 10^{-9}$ Torr for 1 h. The mass spectrum of unweathered gasoline (Figure 5 (top)) consists of ~150 species in the range, $50 \leq m/z \leq 250$, dominated by species in the range, $100 \leq m/z \leq 170$. Compared to unweathered diesel spectra, the gasoline spectrum is much simplified (*60*−*62*), with (usually) one (but up to four) different elemental compositions at each nominal mass. A molecular formula could be assigned to every peak in the broadband mass spectrum with an average error of 0.8 ppm. The 75% weathered gasoline spectrum (Figure 5, bottom) exhibits depletion of various components, but the change is less drastic than for diesel fuel (which is compositionally much more diverse).

Unweathered/Weathered Jet Fuel (JP-8). A 1 μL septum injection of unweathered/weathered jet fuel (JP-8) into the AGHIS led to a stable base pressure of $\sim 5 \times 10^{-9}$ Torr for 1 h. The mass spectrum consisted of ~400 peaks in the range, $50 \leq m/z \leq 250$ with as many as four peaks a single nominal mass. Figure 6 shows the broadband mass spectrum of unweathered jet fuel (bottom) along with a zoom mass inset (top) showing baseline resolution of four peaks at $m/z \sim 154$ at a mass resolving power ($m/\Delta m_{50\%}$) ≈ 100 000. Elemental composition assignment of all the peaks in the mass spectrum was achieved based on accurate mass measurement with an average mass error of 0.4 ppm. Because a large volume of bulk JP-8 fuel was available, we were able to characterize the degree of weathering from 25 to 95% in several increments. Changes in the broadband mass spectrum become readily apparent at >50% weathering and became more pronounced at higher degrees of weathering. Figure 7 shows the broadband mass spectra for both unweathered (top) and 85% weathered (bottom) jet fuel. A shift toward higher relative abundance of higher (>250) m/z components for the 85% weathered fuel is clearly evident, particularly from the zoom mass inset above each broadband spectrum.

As for the diesel fuel analysis, a difference mass spectrum (Figure 8) facilitates comparison of the effect of weathering on composition of JP-8. As for diesel fuel, there are series of negative and positive peaks, with components spaced at ~14 Da apart (CH_2), with preferential evaporative loss of lower-mass components. However, there is again overlap between negative and positive peak mass ranges, indicating that evaporative loss does not completely correlate with mass. Molecular formula assignment of all the peaks in the mass spectrum provides compositional fingerprints for both unweathered and weathered JP-8, thereby allowing for positive identification of JP-8 as a contaminant even after severe weathering.

Compositional Analysis vs Pattern Recognition. Identification of a complex substance which itself consists of multiple components (e.g., gasoline) is a well-studied problem. In various forms of pattern recognition (e.g., principal component analysis (*63*−*65*)) the complex substance is somehow dispersed (e.g., chromatographically or spectroscopically) into a series of signals (e.g., chromatographic peaks). One then seeks to find a particular set of individual peaks whose magnitudes vary in the same

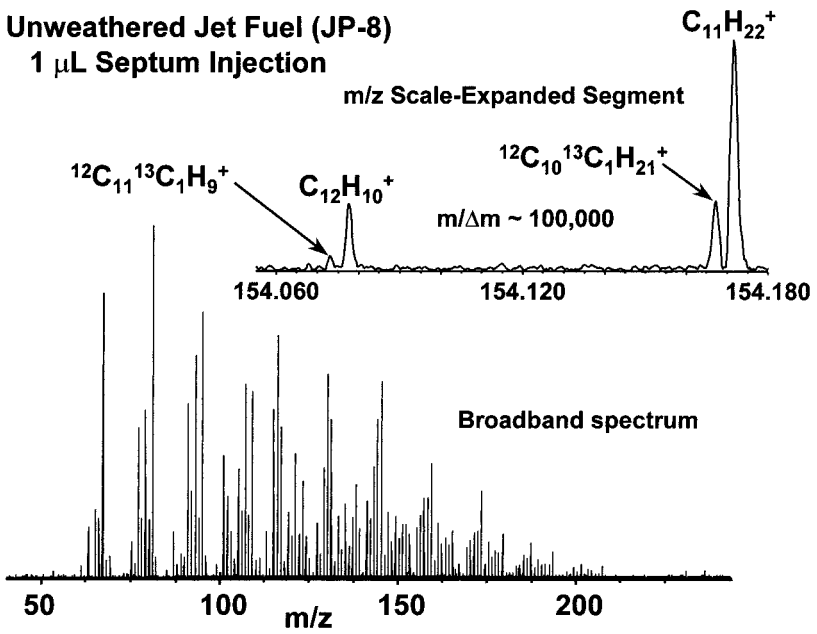

FIGURE 6. Full-range FT-ICR mass spectrum of an unweathered jet fuel (JP-8) sample resulting from a 1 μL septum injection into the AGHIS (bottom). Baseline resolution of four components present at the same nominal mass (inset) is achieved at a mass resolving power ($m/\Delta m_{50\%}$) $\approx$ 100 000.

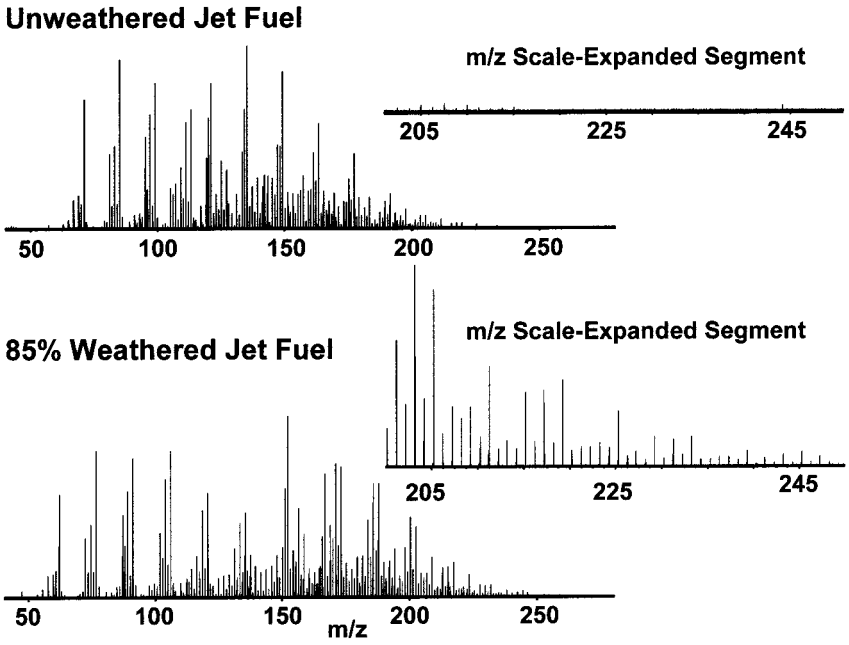

FIGURE 7. Full-range FT-ICR mass spectra for unweathered (top) and 85% weathered (bottom) jet fuel, showing preferential evaporation of lower-mass species as a result of weathering. The increased relative abundance of high-mass components is especially evident from the zoom mass segments shown above each full-range mass spectrum.

proportion when the substance is present at different concentrations. An important feature of principal component analysis is that it does not require identification of the peaks; only their collective pattern for a given substance is needed.

Here, we identify the various components of the complex substance (e.g., different hydrocarbons in gasoline). Thenceforth, the pattern of their relative abundances need no longer be conserved—we can simply search to see if species with the same elemental composition as in the original substance are present. When conventional methods, such as chromatographic peaks, are used to monitor fuel weathering, the resolution of the individual peaks is not sufficient to get a true picture of the chemical/physical changes that occur. The present approach relies on the high resolving power of FT-ICR MS and allows individual components to be resolved and monitored, for a much more specific picture of these changes. It is important to recognize that that approach differs fundamentally from traditional pattern recognition. We propose to extend the present analysis to contamination of laboratory soil containers by fuel oils, crude oils, transportation fuels, and other commercial hydrocarbon solvents followed by solvent extraction and FT-ICR mass spectral analysis.

Acknowledgments

The authors thank Daniel McIntosh for machining all of the custom parts required for the 6 T instrument construction and Randall Pelt for the glasswork on the AGHIS. The authors

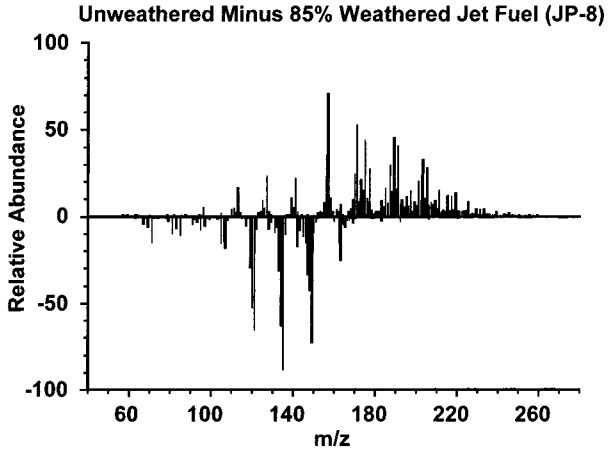

FIGURE 8. Unweathered minus 85% weathered JP-8 jet fuel *m/z* difference spectrum. Weathering clearly results in preferential removal of low-mass species (negative peaks) to leave high-mass species at higher relative abundance (positive peaks).

also thank Christopher L. Hendrickson and John P. Quinn for many helpful discussions and Steve Williams (Eglin AFB) for providing the bulk jet fuel (JP-8). This work was supported by the NSF National High-Field FT-ICR Mass Spectrometry Facility (CHE-94-13008), American Chemical Society Division of Analytical Chemistry graduate fellowship (to RPR) sponsored by the Society of Analytical Chemists of Pittsburgh, Florida State University, and the National High Magnetic Field Laboratory at Tallahassee, FL.

Literature Cited

(1) Dragun, J. *Remediation Techniques Environmental Fate and Risk Assessment*; Kostecki, P. T., Calabrese, E. J., Eds.; Lewis Publishing: Chelsea, MI, 1989; Vol. 1, pp 211−220.
(2) *Petroleum Contaminated Soils*; Lewis Publishers: Chelsea, MI, 1989; Vol. 2.
(3) *Petroleum Contaminated Soils*; Lewis Publishers: Chelsea, MI, 1989; Vol. 1.
(4) Fine, P.; Graber, E. R.; Yaron, B. *Soil Technol.* **1997**, *10*, 133−153.
(5) Mercer, J. W.; Cohen, R. M. *J. Contam. Hydrol.* **1990**, *6*, 107−163.
(6) Yaron, B. *Ecol. Stud.* **1989**, *73*, 211−230.
(7) Yocum, P. S.; Irvine, R. L.; Bumpus, J. A. *Water Environ. Res.* **1995**, *67*, 174−180.
(8) Hillel, D. *Remediation Techniques Environmental Fate and Risk Assessment*; Kostecki, P. T., Calabrese, E. J., Eds.; Lewis Publishing: Chelsea, MI, 1989; Vol. 1, pp 81−86.
(9) Potter, T. L. *Remediation Techniques & Analytical Methodologies*; Kostecki, P. T., Calabrese, E. J., Eds.; Lewis Publishing: Chelsea, MI, 1989; Vol. 2, pp 97−110.
(10) *Energy Resources Separations Manual*; Waters Associates Inc.: Milford, MA, 1978.
(11) E. P. A. *SW846 Test Methods for Evaluating Solid Waste*; E.P.A., Ed.; Environmental Protection Agency: Washington, DC, 1995.
(12) Reemtsma, T.; Mehrtens, J. *Chemosphere* **1997**, *35*, 2491−2501.
(13) Zhang, Z.; Pawliszyn, J. *Anal. Chem.* **1993**, *65*, 1843−1852.
(14) Clement, R. E.; Yang, P. W.; Koester, C. J. *Anal. Chem.* **1997**, *69*, 251R-287R.
(15) Hewitt, A. D.; Miyares, P. H.; Leggett, D. C.; Jenkins, T. F. *Environ. Sci. Technol.* **1992**, *26*, 1932−1938.
(16) Slater, G. F.; Dempster, H. S.; Lollar, B. S.; Ahad, J. *Environ. Sci. Technol.* **1999**, *33*, 190−194.
(17) Novak, J. T. *Monitoring and Verification of Bioremediation*; Hinchee, R. E., Douglas, G. S., Ong, S. K., Eds.; Battelle Press: Columbus, OH, 1995; Vol. 3, pp 29−38.
(18) Dragun, J. *Remediation Techniques & Analytical Methodologies*; Kostecki, P. T., Calabrese, E. J., Eds.; Lewis Publishing: Chelsea, MI, 1989; Vol. 2, pp 149−156.
(19) Kostle, P. A. *Remediation Techniques & Analytical Methodologies*; Kostecki, P. T., Calabrese, E. J., Eds.; Lewis Publishing: Chelsea, MI, 1989; Vol. 2, pp 137−148.
(20) Baumann, B. *Remediation Techniques & Analytical Methodologies*; Kostecki, P. T., Calabrese, E. J., Eds.; Lewis Publishing: Chelsea, MI, 1989; Vol. 2, pp 31−42.
(21) Baumann, B. *Remediation Techniques Environmental Fate & Risk Assessment*; Kostecki, P. T., Calabrese, E. J., Eds.; Lewis Publishing: Chelsea, MI, 1989; Vol. 1, pp 3−20.
(22) Haney, J. *Remediation Techniques & Analytical Methodologies*; Kostecki, P. T., Calabrese, E. J., Eds.; Lewis Publishing: Chelsea, MI, 1989; Vol. 2, pp 55−72.
(23) Tucker, R. K. *Remediation Techniques Environmental Fate and Risk Assessment*; Kostecki, P. T., Calabrese, E. J., Eds.; Lewis Publishing: Chelsea, MI, 1989; Vol. 1, pp 37−54.
(24) Banerjee, D. K.; Gray, M. R. *Environ. Sci. Technol.* **1997**, *31*, 646−650.
(25) Wang, Z.; Fingas, M.; Blenkinsopp, S.; Sergy, G.; Landriault, M.; Sigouin, L.; Lambert, P. *Environ. Sci. Technol.* **1998**, *32*, 2222−2232.
(26) Wang, Z.; Fingas, M.; Sergy, G. *Environ. Sci. Technol.* **1995**, *29*, 2622−2631.
(27) Wang, Z.; Fingas, M. *Environ. Sci. Technol.* **1995**, *29*, 2842−2849.
(28) Wang, Z.; Fingas, M. *Eniviron. Sci. Technol.* **1996**.
(29) Wang, Z.; Fingas, M.; Blenkinsopp, S.; Sergy, G.; Landriault, M.; Sigouin, L.; Foght, J.; Semple, K.; Westlake, D. W. S. *J. Chromatogr. A* **1998**, *809*, 89−107.
(30) Oudot, J.; Merlin, F. X.; Pinvidic, P. *Marine Environ. Res.* **1998**, *45*, 113−125.
(31) Stout, S. A.; Lundegard, P. D. *Appl. Geochem.* **1998**, *13*, 851−859.
(32) Boehm, P. D.; Page, D. S.; Gilfillan, E. S.; Bence, A. E.; Burns, W. A.; Mankiewicz, P. J. *Environ. Sci. Technol.* **1998**, *32*, 567−576.
(33) Douglas, G. S.; Bence, E. A.; Prince, R. C.; McMillen, S. J.; Butler, E. L. *Environ. Sci. Technol.* **1996**, *30*, 2332−2339.
(34) Parker, E. F.; Burgos, W. D. *Environ. Eng. Sci.* **1999**, *16*, 21−29.
(35) Mansuy, L.; Philp, R. P.; Allen, J. *Environ. Sci. Technol.* **1997**, *31*, 3417−3425.
(36) Ma, X.; Sakanishi, K.; Isoda, T.; Mochida, I. *Fuel* **1997**, *76*, 329−339.
(37) Saeed, T.; Al-Hashash, H.; Al-Matrouk, K. *Environment Intl.* **1998**, *24*, 141−152.
(38) Huesemann, M. H. *Eniviron. Sci. Technol.* **1994**, *29*, 7−18.
(39) Huesemann, M. H. *Monitoring and Verification of Bioremediation*; Hinchee, R. E., Douglas, G. S., Ong, S. K., Eds.; Battelle Press: Columbus, OH, 1995; Vol. 3, pp 11−18.
(40) Huesemann, M. H. *Environ. Sci. Technol.* **1995**, *29*, 7−18.
(41) McLafferty, F. W. *Acc. Chem. Res.* **1994**, *27*, 379−386.
(42) Wilkins, C. L. *Trends in Analytical Chemistry 13, Special Issue: Fourier Transform Mass Spectrometry*; Wilkins, C. L., Ed.; 1994; pp 223−251.
(43) Freiser, B. S. *J. Mass Spectrom.* **1996**, *31*, 703−715.
(44) Marshall, A. G. *International Journal of Mass Spectrometry Ion Processes 137/138: Special Issue: Fourier Transform Ion Cyclotron Resonance Mass Spectrometry*; Marshall, A. G., Ed., 1996; p 410.
(45) Marshall, A. G.; Hendrickson, C. L.; Jackson, G. S. *Mass Spectrom. Rev.* **1998**, *17*, 1−35.
(46) Dienes, T.; Pastor, S. J.; Schürch, S.; Scott, J. R.; Yao, J.; Cui, S.; Wilkins, C. L. *Mass Spectrom. Rev.* **1996**, *15*, 163-211.
(47) Amster, I. J. *J. Mass Spectrom.* **1996**, *31*, 1325−1337.
(48) Laude, D. A.; Stevenson, E.; Robinson, J. M. *Electrospray Ionization Mass Spectrometry*; Cole, R. B., Ed.; John Wiley & Sons: New York, 1997; pp 291−319.
(49) Rodgers, R. P.; White, F. M.; Hendrickson, C. L.; Marshall, A. G.; Andersen, K. V. *Anal. Chem.* **1998**, *70*, 4743−4750.
(50) Rodgers, R. P.; White, F. M.; McIntosh, D. G.; Marshall, A. G. *Rev. Scientific Instrum.* **1998**, *69*, 2278−2284.
(51) Guan, S.; Marshall, A. G.; Scheppele, S. E. *Anal. Chem.* **1996**, *68*, 46−71.
(52) Senko, M. W.; Canterbury, J. D.; Guan, S.; Marshall, A. G. *Rapid Commun. Mass Spectrom.* **1996**, *10*, 1839−1844.
(53) Littlejohn, D. P.; Ghaderi, S., U.S.A. Patent No. 4,581,533, issued 8 April, 1986.
(54) Stafford, C.; Morgan, T. D.; Brunfeldt, R. J. *Int. J. Mass Spectrom. Ion Proc.* **1968**, *1*, 87−92.
(55) Rodgers, R. P.; Blumer, E. N.; Freitas, M. A.; Marshall, A. G. *Submitted to Anal. Chem.* **1999**.
(56) Ledford, E. B., Jr.; Rempel, D. L.; Gross, M. L. *Anal. Chem.* **1984**, *56*, 2744−2748.
(57) Wise, M. B. *Anal. Chem.* **1987**, *59*, 2289−2293.
(58) Kondrat, R. W. *Tandem Mass Spectrometry*; McLafferty, F. W., Ed.; John Wiley & Sons: New York, Chichester, Brisbane, Toroton, Singapore, 1983; pp 474−490.

(59) McLafferty, F. W. *Tandem Mass Spectrometry*; McLafferty, F. W., Ed.; Wiley: New York, 1983.
(60) Brown, R. A. *Anal. Chem.* **1951**, *23*, 430−437.
(61) Lumpkin, H. E.; Johnson, B. H. *Anal. Chem.* **1954**, *26*, 1719−1722.
(62) Aczel, T.; Allan, D. E.; Harding, J. H.; Knipp, E. A. *Anal. Chem.* **1970**, *42*, 341−347.
(63) Massart, D. L.; Vandeginste, B. G. M.; Buydens, L. M. C.; De Jong, S.; Lewi, P. J.; J., S.-V. *Handbook of Chemometrics and Qualimetrics*; Elsevier: Amsterdam, 1998.
(64) Jurs, P. C. *Chemical Applications of Pattern Recognition*; Wiley: New York, 1975.
(65) Joliffe, I. T. *Principal Component Analysis*; Springer-Verlag: New York, 1986.

Received for review July 16, 1999. Revised manuscript received December 21, 1999. Accepted January 27, 2000.

ES990799I